Time delay comb transducers for aircraft inspection

F. Yan
fzy101@psu.edu
Department of Engineering Science and Mechanics
Pennsylvania State University, PA
USA

J. L. Rose
jlresm@engr.psu.edu
Department of Engineering Science and Mechanics
Pennsylvania State University, PA
USA

FBS Inc
State College, PA
USA

ABSTRACT

An ultrasonic guided wave technique based on time delay comb transducers is introduced for aircraft inspection. It is demonstrated that for isotropic plate structures the time delay comb transducers with appropriate excitation are capable of performing discontinuity detections without knowing the precise isotropic material properties of the objects being inspected. Fibre-reinforced composite plates are also considered. The wave skew effects are investigated using both the slowness curve and the Poynting vector. A composite inspection technique that takes advantage of the skew effects is proposed. Using time delay comb transducers to excite the guided wave modes with different skew angles, the proposed technique is capable of scanning the composite plate in different directions without moving or rotating the transducers. By contrast with the applications in the isotropic cases, knowledge of the material properties and other necessary information that is needed to produce dispersion curves is generally required. Experimental results are provided as a validation of the proposed techniques.

NOMENCLATURE

a	comb transducer element width
A	amplitude factor
d	distance between adjacent comb elements
$\hat{\mathbf{e}}$	unit vector in the wave propagation direction
$\mathbf{E}$	excitation spectrum
$\mathbf{E}_z^{overall}$	overall z direction excitation spectrum of a comb transducer
$\mathbf{E}_z^{TD}$	time delayed excitation spectrum for forward propagating waves
$\mathbf{E}_z^{TD}$	time delayed excitation spectrum for backward propagating waves
f_0	centre frequency of the comb transducer
h	plate thickness
H	heaviside step function
k	wave number
m	number of cycles
N	number of elements
$\mathbf{P}$	acoustic Poynting vector
$P_{\nu\mu}$	orthogonal relation between the ν th and the μ th guided wave modes
s	tone-burst signal
S	fourier spectrum of the tone-burst signal
$\mathbf{t}$	traction distribution
t	time
t_0	time duration of the tone-burst signal
$\underline{\mathbf{T}}$	stress field
$\overline{\mathbf{T}}$	stress distribution across the plate thickness
$\tilde{\mathbf{T}}$	complex conjugate of the stress field
$\mathbf{u}$	particle displacement vector
$\overline{\mathbf{u}}$	wave structure
$\mathbf{v}$	particle velocity vector
$\overline{\mathbf{v}}$	particle velocity distribution across the plate thickness
$\tilde{v}$	complex conjugate of the particle velocity vector
x	cartesian co-ordinate for the wave propagation direction
y	cartesian co-ordinate for the plate width direction
z	cartesian co-ordinate for the plate thickness direction
φ_{skew}	skew angle
μ,ν	guided wave modes
ω	circular frequency
ω_0	centre circular frequency
τ	time delay

Paper No. 3353. Manuscript received 7 October 2008, accepted 17 December 2008.

https://doi.org/10.1017/S0001924000003080 Published online by Cambridge University Press

1.0 INTRODUCTION

The aircraft industry has experienced an increasing demand on reliable and cost effective inspection techniques to ensure aviation safety. Ultrasonic guided wave based techniques have been more and more involved in the aircraft inspection field in recent years[1-6]. Ultrasonic guided waves have a capability of following the contours of the wave guides and propagating over long distances, which makes them quite suitable for aircraft inspection, since time consuming point-to-point tests can be avoided when using the guided wave techniques. Moreover, the great variations of guided wave displacement and stress distributions offer us excellent flexibility for selecting specific wave modes and frequencies to meet different inspection requirements[7]. To take advantage of this flexibility, however, various guided wave transducer designs are needed to target the selected wave modes and frequencies. Various guided wave transducers including angle wedge transducers[8], piezoelectric wafer active sensors (PWAS)[9-10], and comb type transducers[11-14] have been developed based on source influence studies. The normal mode expansion method, used in the source influence study[8], suggests that guided wave excitation can be considered as a combination of the guided wave excitability, which is the intrinsic characteristic of the guided wave mode and the excitation spectrum determined by the properties of the applied source. In Refs 12-14, it is shown that the excitation spectrums of the comb type transducers can be varied by applying time delays to the comb elements. Guided wave mode tuning can thus be achieved with a time delay profile adjustment across the comb elements. In this paper, we discuss the excitation spectrum variations with respect to the time delays in order to apply the time delay comb transducers to the detection of discontinuities in isotropic plate structures whose material properties and thicknesses are unknown. To move one step further, the time delay comb transducers are also applied to the inspections of fibre-reinforced composite materials.

The use of fibre-reinforced composite materials on aircraft has grown steadily since the first glass fibre laminate fuselage was built in 1944[15]. Composite materials offer many benefits over monolithic materials in the aircraft industry, such as light weight, high strength, high stiffness, long fatigue life, corrosion resistance, etc[16]. However, from a nondestructive evaluation (NDE) or structural health monitoring (SHM) point of view, the use of composite materials makes the inspections of the aircraft more complex. Fibre-reinforced composite materials are mechanically anisotropic. The anisotropy of the composite materials introduces guided wave skew effects upon which the energy propagation direction does not necessary coincide with the wave launching direction[17-19]. Obviously, the wave skew effects need to be taken into consideration when utilising guided waves for composite inspections. In general, the guided wave skew effects are considered undesirable in guided wave inspections. To avoid them, wave propagation in the material symmetric directions or guided wave modes and frequencies that are almost immune to the material anisotropy (referred as quasi-isotropic mode points in Ref. 20) must be selected. In this paper, by contrast, we propose to make use of the guided wave skew effects instead of avoiding them in the composite inspections. By choosing guided wave modes and frequencies to obtain different skew angles, the guided wave energies are sent into different directions although the wave launching direction remains unchanged. The time delay comb transducers serve as the means of guided wave mode selection in our proposed technique, because the guided wave skew angle tuning can be fulfilled electronically using the time delay comb transducers.

This paper is organised as follows. In the next section, the basics of guided wave propagation and excitation in isotropic plate wave guides are briefly reviewed. The concepts of a guided wave excitability and excitation spectrum are introduced. The excitation spectrums for time delay comb transducers are investigated in Section 3. The feasibility of guided wave mode tuning using the time delay comb transducer is demonstrated in this section as well. Using an aluminium plate as an example, the excitation spectrum calculations are experimentally validated in Section 4. The time delay tuning processes that can be taken to achieve blind discontinuity detection (discontinuity detection without knowing the material properties and plate thickness) in isotropic plate structures are presented in Section 5. Section 6 focuses on the wave skew effects in fibre-reinforced composite plates. The skew angle dispersion curves are calculated based on the directions of the Poynting vectors with respect to the wave launching directions. The skew angle tuning of guided waves in composite plates using the time delay comb transducers can then be conducted on the basis of the excitation spectrums and the skew angle dispersion curves. In Section 7, experimental results on an aluminium plate are presented first. The idea of employing the time delay comb transducers to inspect plates without knowing their dispersion curves is presented. Following that, the experimental results on the skew angle tuning are given. A feasibility study on defect detection using the skew angle tuning is also provided. At last, some concluding remarks and future directions are given in Section 8.

2.0 GUIDED WAVE PROPAGATION AND EXCITATION IN ISOTROPIC PLATES

The problem of guided wave propagation in traction free isotropic plates has been well addressed in the literature[7,21]. The problem geometry is depicted in Fig. 1, in which x is in the wave propagation direction and z is in the plate thickness direction. The width of the plate is assumed to be infinite in the y direction such that the plane strain assumption is used when solving the problem. It has been demonstrated that the plane harmonic guided wave solutions for a traction free plate are of the form:

$$\mathbf{u}_\nu(x,z,t) = A_\nu(x)\overline{\mathbf{u}}_\nu(z)e^{i(\omega t - k_\nu x)}, \qquad \ldots (1)$$

where $\mathbf{u}$ represents the particle displacement field, A represents the amplitude factor, $\overline{\mathbf{u}}$ represents the displacement distributions across the thickness of the plate (often referred as wave structure or mode shape), k denotes the wavenumber, the subscript ν denotes the νth guided wave mode, and ω denotes the circular frequency. In the Lamb wave solutions, the vectors $\mathbf{u}$ and $\overline{\mathbf{u}}$ have nonzero x and z components, whereas in the shear horizontal (SH) wave solutions, the only nonzero components are the y components. The wavenumber k in Equation (1) is a function of the circular frequency ω. Different guided wave modes bear different dispersion relations between the wavenumber and the frequency. The comprehensive representation of the dispersion relations is usually given by the dispersion curves. The wave structures described by the vector $\overline{\mathbf{u}}$ vary significantly for different guided wave modes and frequencies. Since different wave structures are suitable for different inspection purposes[7], the variation of the vector $\overline{\mathbf{u}}$ produces a great flexibility when developing guided wave based inspection techniques.

It is important to know that the guided wave modes are orthogonal to each other at any given frequency. The orthogonality shown as follows has been proven based on the complex reciprocity relation[21].

$$P_{\nu\mu} = -\frac{1}{4}\int_{-h/2}^{h/2}\left(\tilde{\mathbf{v}}_\nu \bullet \mathbf{T}_\mu + \mathbf{v}_\mu \bullet \tilde{\mathbf{T}}_\nu\right)\bullet \hat{\mathbf{e}}_x dz \qquad \ldots (2)$$

$$P_{\nu\mu} = 0, \text{ unless } \nu = \mu\,. \qquad \ldots (3)$$

In Equations (2) and (3), $\mathbf{v}$ and $\mathbf{T}$ are the particle velocity vector and the stress field, respectively. The tilde denotes complex conjugation. The subscript letters ν and μ represent the νth and the μth guided wave modes, respectively. The unit vector that points to the

https://doi.org/10.1017/S0001924000003080 Published online by Cambridge University Press

wave propagation direction is denoted by $\hat{\mathbf{e}}_x$. The thickness of the plate is h, as shown in Fig. 1. Due to the orthogonality and also the completeness[22] of the guided wave modes, any guided wave field can be expanded into a combination of different guided wave modes:

$$\mathbf{v}(x,z) = \sum_{\nu} A_{\nu}(x)\overline{\mathbf{v}}_{\nu}(z)e^{-ik_{\nu}x}, \quad \ldots (4)$$

$$\mathbf{T}(x,z) = \sum_{\nu} A_{\nu}(x)\overline{\mathbf{T}}_{\nu}(z)e^{-ik_{\nu}x}. \quad \ldots (5)$$

The harmonic time dependence of the guided wave fields are dropped here for brevity. The amplitude factors of all guided wave modes under a certain wave excitation source can be determined using the reciprocity relation together with the orthogonality[8]. For wave excitation sources that are applied to the top surface of the plate, the amplitude factors can be calculated as;

$$A_{\nu}(x) = \frac{e^{-ik_{\nu}x}}{4P_{\nu\nu}}\tilde{\mathbf{v}}_{\nu}(h/2)\bullet\int_{-\infty}^{\infty}\mathbf{t}(x)e^{ik_{\nu}x}\mathrm{d}x, \quad \ldots (6)$$

with $\mathbf{v}_{\nu}(h/2)$ representing the particle velocity vector of the νth mode at the top surface of the plate and $\boldsymbol{t}$ representing the traction distribution of the source in the x direction.

It is clear that the magnitude of the amplitude factors given in Equation (6) can be written as the dot product of two terms:

$$|A_{\nu}| = \underbrace{\left|\frac{\tilde{\mathbf{v}}_{\nu}(h/2)}{4P_{\nu\nu}}\right|}_{term1}\bullet\underbrace{\left|\int_{-\infty}^{\infty}\mathbf{t}(x)e^{ik_{\nu}x}\mathrm{d}x\right|}_{term2}. \quad \ldots (7)$$

The *term* 1 in Equation (7) is the excitability of the guided wave mode that is independent of the traction distribution. The *term* 2 is considered as the excitation term determined by the traction distribution. Because the excitation term can be related to the spatial Fourier transform of the traction distribution **t** by the following equation:

$$\int_{-\infty}^{\infty}\mathbf{t}(x)e^{ik_{\nu}x}\mathrm{d}x = \left(\int_{-\infty}^{\infty}\mathbf{t}(x)e^{ikx}\mathrm{d}x\right)_{k=k_{\nu}}, \quad \ldots (8)$$

a general wavenumber space excitation spectrum which is independent of guided wave modes can be defined as the magnitude of the spatial Fourier transform:

$$\mathbf{K}(k) = \left|\int_{-\infty}^{\infty}\mathbf{t}(x)e^{ikx}\mathrm{d}x\right|. \quad \ldots (9)$$

For transient wave excitation sources, the frequency bandwidth of the excitation signal also affects the guided wave excitation. Hence, the excitation spectrum is modified to include the Fourier transform of the excitation signal:

$$\mathbf{E}(k,\omega) = \mathbf{K}(k)|S(\omega)|, \quad \ldots (10)$$

where $S(\omega)$ denotes the Fourier transform of the time domain excitation signal.

3.0 EXCITATION SPECTRUMS OF TIME DELAY COMB TRANSDUCERS

To investigate the excitation spectrums of time delay comb transducers, we start with the conventional comb type transducers with no

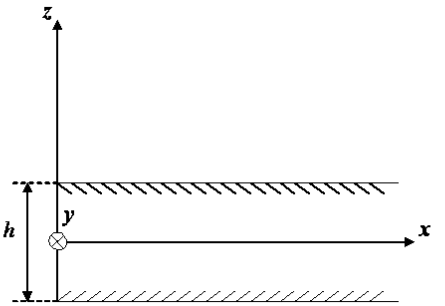


Figure 1. Problem geometry of guided wave propagation in plates.

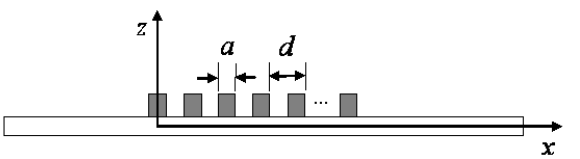


Figure 2. Illustration of a conversional comb type transducer.

time delays. As illustrated in Fig. 2, the element width of the comb transducer is a and the distance between adjacent elements is d.

Assuming that each comb element produces a uniform out-of-plane loading, one can then express the traction distribution of the very left element shown in Fig. 2 as:

$$\mathbf{t}(x) = f_0\hat{\mathbf{e}}_z, -a/2 \le x \le a/2\,. \quad \ldots (11)$$

Since the applied traction is in the z direction only, we focus on the excitation spectrum for the z direction, i.e., $\mathbf{E}_z(k,\omega)$ The traction distribution given in Equation (11) is a rectangular function. It is easy to show that the spatial Fourier transform of this function yields:

$$\mathbf{K}_z(k) = f_0\left|\frac{\mathrm{Sin}(ka/2)}{k/2}\right| \quad \ldots (12)$$

A m cycle tone-burst signal can be expressed as:

$$s(t) = [H(t) - H(t-t_0)]e^{i\omega_0 t}, \quad \ldots (13)$$

where $H(t)$ is the Heaviside step function, t_0 is the time duration of the tone-burst signal, and ω_0 is the centre circular frequency of the signal. If this signal is used as the wave excitation signal, the function $S(\omega)$ as the Fourier transform of $s(t)$ becomes:

$$S(\omega) = \frac{\mathrm{Sin}[(\omega-\omega_0)m/2\omega_0]}{(\omega-\omega_0)/2}. \quad \ldots (14)$$

Thus, the excitation spectrum of the single element centreed at $x = 0$ can be calculated as:

$$\mathbf{E}_z(k,\omega) = f_0\left|\frac{\mathrm{Sin}(ka/2)}{k/2}\frac{\mathrm{Sin}[(\omega-\omega_0)m/2\omega_0]}{(\omega-\omega_0)/2}\right|. \quad \ldots (15)$$

For conversional comb type transducers, all of the elements are excited at the same time. The magnitudes of the excitation spectrums for all elements are the same. However, there are phase differences. The phase differences among the waves excited by different elements arise from the element location differences. When combining the excitation spectrums of all elements to yield the

https://doi.org/10.1017/S0001924000003080 Published online by Cambridge University Press

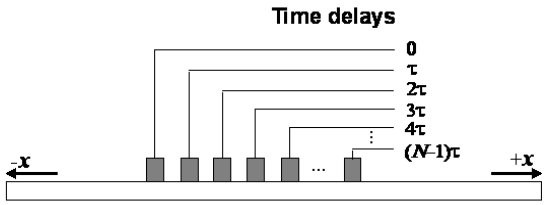
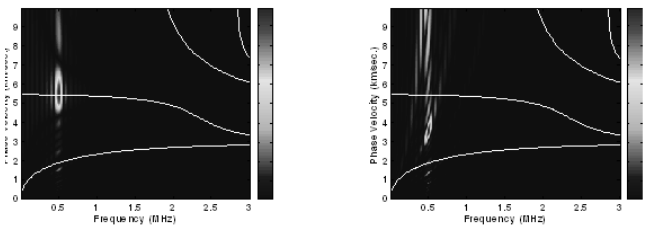


Figure 3. Illustration of a time delay comb transducer.



(a) $+x$ wave propagation direction (b) $-x$ wave propagation direction

Figure 4. Excitation spectrums of a time delay comb transducer.

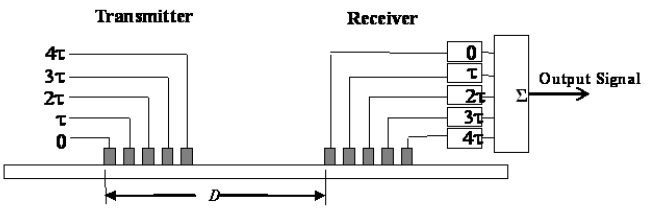


Figure 5. Time delay comb transducers working under a pitch-catch mode.

overall excitation spectrum of the comb transducer, one needs to add in the summation of the phase difference terms which is given as:

$$\sum_{n=0}^{N-1} e^{ikdn} = \frac{\mathrm{Sin}(kdN/2)}{\mathrm{Sin}(kd/2)} e^{i\frac{kd}{2}(N-1)}, \quad \ldots (16)$$

for a N element comb transducer. Therefore, after normalisation, the overall excitation spectrum of a N element comb transducer driven by a m cycle tone-burst excitation signal can be expressed as:

$$\mathbf{E}_z^{overall}(k,\omega) = \left| \frac{\mathrm{Sin}(ka/2)}{k/2} \frac{\mathrm{Sin}(kdN/2)}{\mathrm{Sin}(kd/2)} \frac{\mathrm{Sin}[(\omega-\omega_0)m/2\omega_0]}{(\omega-\omega_0)/2} \right|. \quad \ldots (17)$$

The illustration of a time delay comb transducer is presented in Fig. 3. As illustrated, the time delays ranging from 0 to $(N-1)\tau$ in an increment step of τ are respectively applied to the N elements from the left to the right in the $+x$ direction. Compared to the conventional comb transducer, the introduction of time delays to the transducer elements only modifies the summation of the phase difference terms as shown in Equation (16). The modified summation is:

$$\sum_{n=0}^{N-1} e^{ikdn} e^{-in\omega\tau} = \frac{\mathrm{Sin}((kd-\omega\tau)N/2)}{\mathrm{Sin}((kd-\omega\tau)/2)} e^{i\frac{kd-\omega\tau}{2}(N-1)}. \quad \ldots (18)$$

As a result, the corresponding normalised excitation spectrum for the time delay comb transducer can be written as:

$$\mathbf{E}_z^{TD}(k,\omega) = \left| \frac{\mathrm{Sin}(ka/2)}{k/2} \frac{\mathrm{Sin}((kd-\omega\tau)N/2)}{\mathrm{Sin}((kd-\omega\tau)/2)} \frac{\mathrm{Sin}[(\omega-\omega_0)m/2\omega_0]}{(\omega-\omega_0)/2} \right|. \quad \ldots (19)$$

It should be noticed that Equation (19) is valid only for the waves propagating in the $+x$ direction. The excitation spectrum for the waves that propagate in the $-x$ direction can be obtained by simply replacing the time delay τ in Equation (19) with $-\tau$:

$$\mathbf{E}_z^{TD'}(k,\omega) = \left| \frac{\mathrm{Sin}(ka/2)}{k/2} \frac{\mathrm{Sin}((kd+\omega\tau)N/2)}{\mathrm{Sin}((kd+\omega\tau)/2)} \frac{\mathrm{Sin}[(\omega-\omega_0)m/2\omega_0]}{(\omega-\omega_0)/2} \right|. \quad \ldots (20)$$

The distinction between Equation (19) and Equation (20) makes it possible to achieve one directional wave excitation using time delay comb transducers[13]. Equation (19) and Equation (20) become identical when $\tau = 0$. Hence, the conventional comb transducers with no time delays have the same excitation spectrums for the waves propagating in opposite directions. This bi-directional wave excitation of the conventional comb transducers is often considered undesired in guided wave inspections.

The examples of the excitation spectrums for a 5 element time delay comb transducer are given in Fig. 4. The element width of the transducer is 4·22mm and the element spacing d is 8·44mm. The excitation signals are 8 cycle tone-burst signals with a centre frequency of 0·5MHz. The time delay τ = 1·56μs . The k-ω domain spectrums are mapped to the frequency-phase velocity domain for the ease of comparison with the phase velocity dispersion curves. The excitation spectrum for the $+x$ wave propagation direction calculated from Equation (19) is shown in Fig. 4 (a), and the one for the $-x$ wave propagation direction calculated from Equation (20) is shown in Fig. 4 (b). The phase velocity dispersion curves of a 1mm thick aluminium plate are plotted in the figures using white lines. As demonstrated, the two excitation spectrums are quite different. With the applied time delays, the comb transducer can well excite the S0 wave mode in a 1mm thick aluminium plate for the $+x$ wave propagation direction. However, the wave excitation for the $-x$ wave propagation direction is much weaker. A one directional wave excitation is thus achieved.

4.0 TIME DELAY COMB TRANSDUCER EXPERIMENT ON AN ALUMINIUM PLATE

Time delay comb transducer experiments were first conducted on an aluminium plate to verify the excitation spectrum calculation and also to study the feasibility of inspecting plates with unknown properties or thicknesses by time delay tuning. Two five element comb transducers were fabricated and used in the experiment in a pitch-catch mode. The element width and element spacing of the two transducers are the same as the ones used for calculating the excitation spectrums shown in Fig. 4: a = 4·22mm and d = 8·44mm. An eight channel time delay control system that can work in both pitch-catch and pulse-echo modes was used to implement the time delays. In the pitch-catch mode, the signals received by the elements of the receiver were delayed and summed in a post-processing fashion. The time delays used for the received signals are the same as the ones applied to the elements of the transmitter, as illustrated in Fig. 5.

The two transducers were placed 250mm apart (D = 250mm) on the surface of a 1mm thick aluminium plate. The excitation tone-burst signals used in the experiment were 8 cycle 0·5MHz tone-bursts. The guided wave signals were recorded for different time delay values. Example signals for the τ values of 0·36μs, 0·84μs, 1·56μs, and 2·04μs are given in Figs 6(a) to (d), respectively.

https://doi.org/10.1017/S0001924000003080 Published online by Cambridge University Press

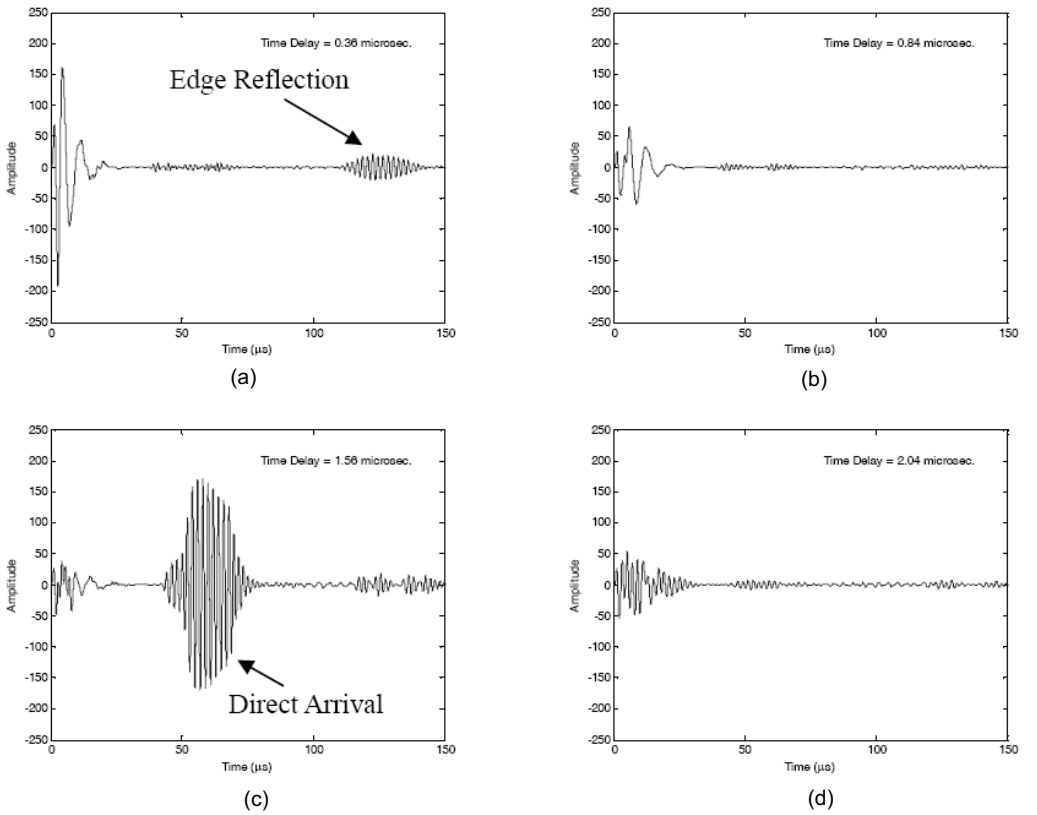


Figure 6. Guided wave signals for the τ values of (a) 0·36μs, (b) 0·84μs, (c) 1·56μs, and (d) 2·04μs.

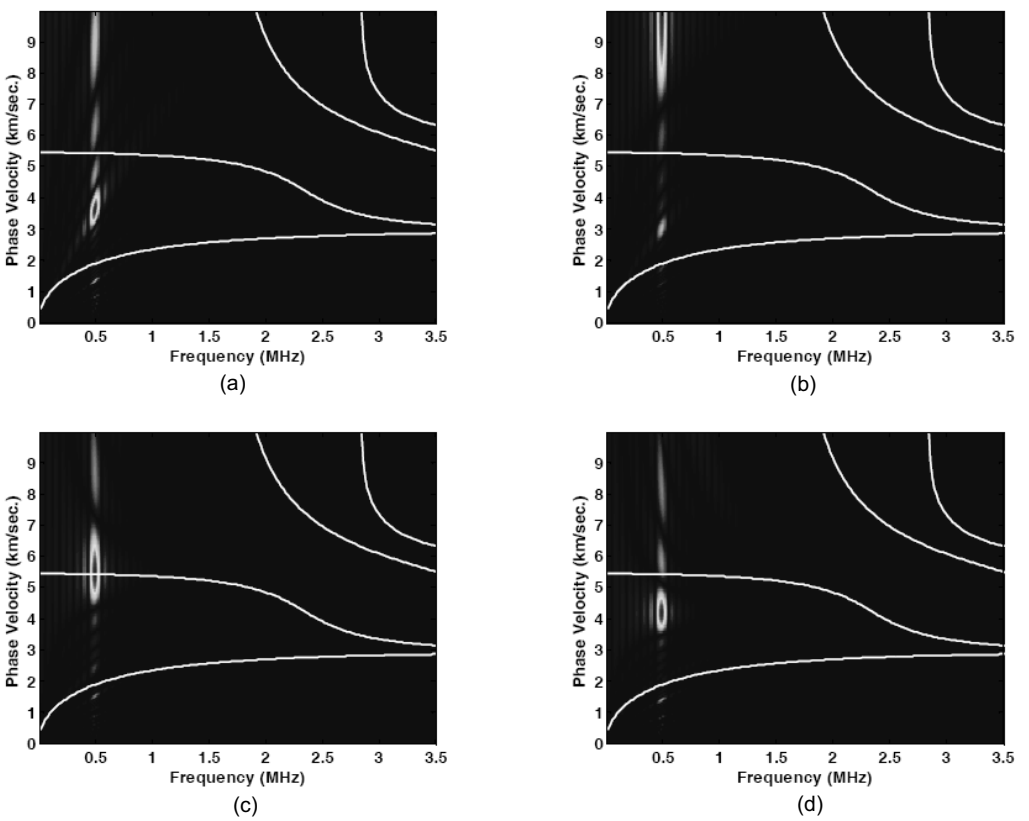


Figure 7. Excitation spectrums for the forward propagating waves. The τ values are: (a) 0·36μs, (b) 0·84μs, (c) 1·56μs, and (d) 2·04μs.

https://doi.org/10.1017/S0001924000003080 Published online by Cambridge University Press

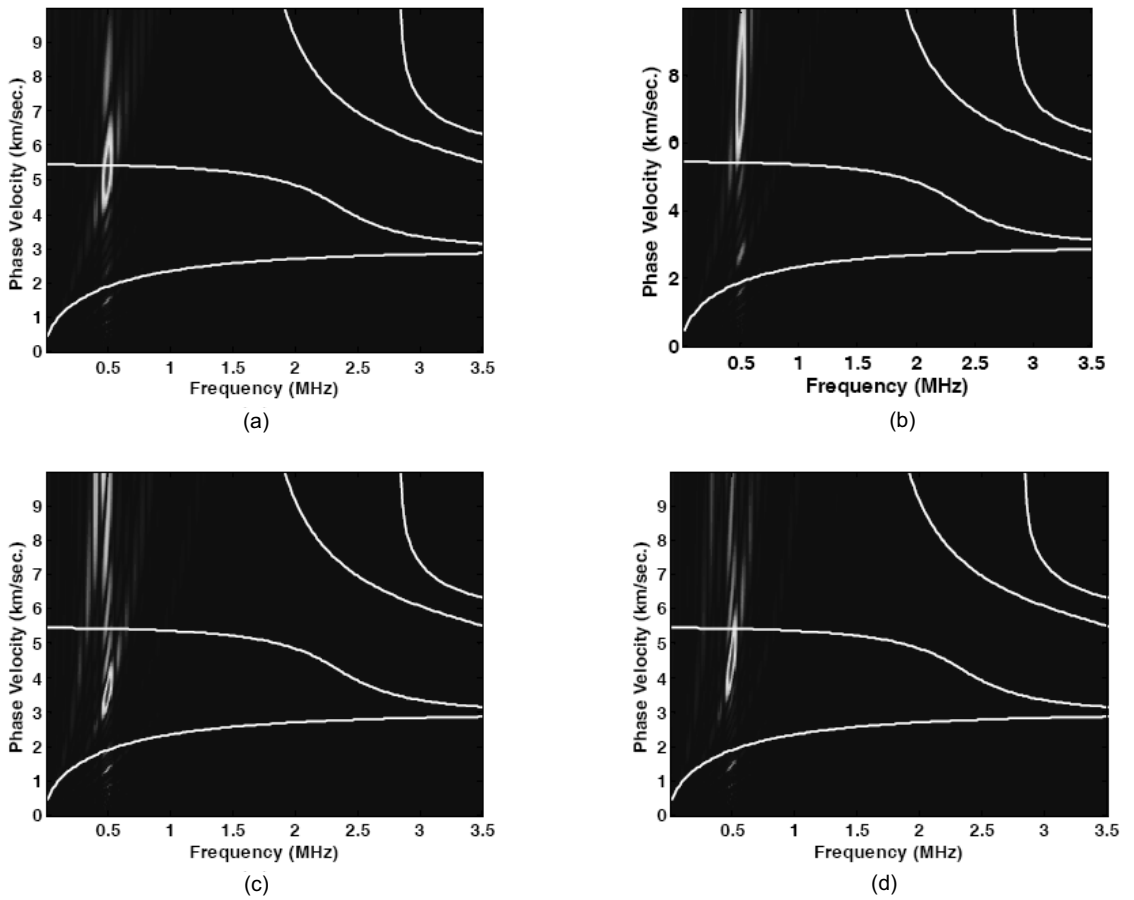


Figure 8. Excitation spectrums for the backward propagating waves. The τ values are: (a) 0·36μs, (b) 0·84μs, (c) 1·56μs, and (d) 2·04μs.

As can be seen, the guided wave signal changed significantly from one time delay profile to another. Clear wave packages were observed when the τ values of 0·36μs and 1·56μs were used. However, the time-of-flights (TOFs) for the observed wave packages are different, as shown in Figs 6 (a) and (c). To interpret the signals, let us look at the excitation spectrums.

As mentioned previously, for one time delay profile, there are two different excitation spectrums for waves that propagate in the opposite directions. Define the direction from left to right in Fig. 5 as the forward propagating direction and the opposite direction as the backward propagating direction. The excitation spectrums for the forward propagating waves were calculated for the time delay values that were applied to obtain the signals shown in Fig. 6. The calculated results are shown in Fig. 7. The corresponding excitation spectrums for the backward propagating waves are presented in Fig. 8. The dispersion curves for the 1mm thick aluminium plate are plotted as backgrounds for all of the figures. It is shown in Fig. 7(a) that the centre of the excitation zone (red area) for the forward propagating waves is away from both the A0 mode and the S0 mode when using the time delay $\tau = 0{\cdot}36\mu s$. For the same time delay value, however, the excitation zone for the backward propagating waves appears on the S0 mode, as shown in Fig. 8 (a). Therefore, the backward propagating S0 mode can be excited. Based on the group velocity of the S0 mode and the TOF, it is determined that the wave package observed in Fig. 6(a) is due to the reflection of the backward propagating S0 mode at the left edge of the plate.

By contrast, for the time delay $\tau = 1{\cdot}56\mu s$, the excitation spectrums shown in Fig. 7(c) and Fig. 8(c) suggest a strong excitation of the forward propagating wave but a weak excitation of the backward propagating wave. This is verified by the signal shown in Fig. 6(c). The direct arrival of the forward propagating wave is clearly shown in the signal whereas only a weak signal is presented at the TOF for the edge reflection of the backward propagating wave.

The excitation spectrums shown in Figs 7(b), (d) and Figs 8(b), (d) demonstrate that the guided wave excitations for both the forward propagating and the backward propagating waves are weak when using the time delays 0·84μs and 2·04μs. As a result, no clear guided wave packages were received when the time delays were applied.

5.0 BLIND DISCONTINUITY DETECTION USING TIME DELAY COMB TRANSDUCERS

Although the material and thickness of the plate were known in the experiment, the results shown in Figs 6-8, to some extent, prove the feasibility of using the time delay comb transducer to inspect plates without knowing their material properties and thicknesses. As demonstrated in Figs 7 and 8, the excitation zone of a time delay comb transducer can be moved around in the frequency-phase velocity domain by applying different time delay profiles, i.e., by using different τ values. Once the centre of the excitation zone locates a guided wave mode in the dispersion curves, the amplitude of the guided wave mode reaches a maximum. The amplitude variation of the direct arrival shown in Fig. 6 is plotted against the applied τ values in Fig. 9. As shown, the τ values for sufficiently selecting the guided wave modes can be easily identified.

https://doi.org/10.1017/S0001924000003080 Published online by Cambridge University Press

Using the through-transmission setup shown in Fig. 5, one can carry out the discontinuity inspection of an unknown plate with a time delay tuning process described as follows.

- Place the comb array transducers onto the plate to be inspected as illustrated in Fig. 5. The distance between the transmitter and the receiver, D, should be at least several wavelengths long to allow the guided waves to form. In a blind test in which the wavelengths are unknown, a D value of 200mm is usually enough.
- Apply time delays to the comb array elements according to Fig. 5. The time delay tuning is achieved by increasing the τ value starting from 0 with a small increment. The output signal from the receiver is recorded for each step of the τ value increment. The time delay tuning is finished once the τ value researches the time delay limit of the time delay circuit.
- After the time delay tuning, it is important to distinguish the direct arrivals of the forward propagating waves from the reflections of the backward propagating waves. If the transmitter is placed away from any reflectors for the guided waves, the direct arrivals of the forward propagating waves can be well separated from all of the reflections of the backward propagating waves. However, in practical applications, sometimes it is difficult to avoid close reflectors for the transmitter. In such cases, we can perform the time delay tuning again with the positions of the transmitter and receiver switched. The TOFs of the direct arrivals remain unchanged in the second time delay tuning. Whereas for the reflections of the backward propagating waves, the wave packages either vanish in the received signals or appear at different TOFs because the conditions for the wave reflections are changed in the second time delay tuning. The wave packages of the direct arrivals can hence be identified.
- The next step is to find the optimum time delay profile for the discontinuity detection of the plate. One can simply choose the time delay profile by which the transducers yield the maximum amplitude for the direct arrival signals as the optimum time delay setting. Using a pulse-echo mode with the optimum time delay profile, the comb array transducer can then be applied to discontinuity detection.
- Since the distance between the two transducers in the through-transmission test is known and the TOF of the guided wave package is available in the received signal, the group velocity of the selected guided wave mode can be easily obtained. As a result, the locations of the discontinuities in the plate can be determined based on the TOFs of the guided wave reflections.

6.0 GUIDED WAVES IN FIBRE-REINFORCED COMPOSITE PLATES

The fibre-reinforced composite plates discussed in this paper are the plates made from unidirectional prepregs using the ply lay-up technique. As the mixture of two distinct materials: fibre and resin, the fibre-reinforced composite plate is inhomogeneous in nature. Nevertheless, for the problem of guided wave propagation in a fibre-reinforced composite plate, when the wavelengths are significantly larger than the fibre diameter and spacing, each layer of the composite plate can be approximately treated as an anisotropic but homogeneous layer. The fibre-reinforced composite plate is hereby considered as a multilayer anisotropic wave guide. Guided wave propagation in such a wave guide can be modeled using various methods including the transfer matrix method[23], the global matrix method[24-25], and the semi-analytical finite element (SAFE) method[26].

The guided wave modes in composite plates can still be represented by Equation (1). Unlike in the isotropic plates, the vectors $\mathbf{u}$ and $\underline{\mathbf{u}}$ of guided wave modes in composite plates may both have three nonzero components if the wave vector direction (x direction)

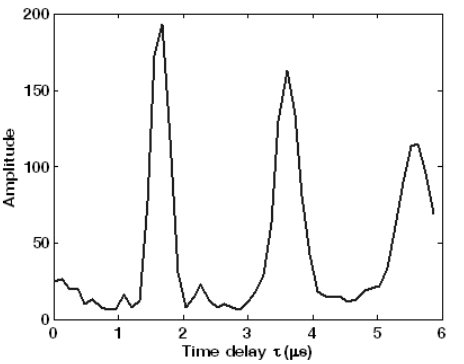


Figure 9. Amplitude variations with respect to the time delay changes.

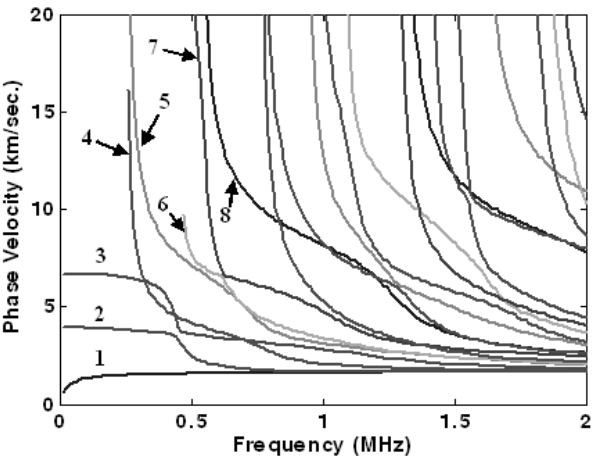


Figure 10. Dispersion curves of the 16 layer quasi-isotropic composite plate for the 0° wave launching direction.

Table 1
Material properties of Cytec CYCOM 977-3 carbon epoxy prepreg

E_1	172 GPa
$E_2 = E_3$	9·8 GPa
G_{23}	3·2 GPa
$G_{12} = G_{13}$	6·1 GPa
ν_{23}	0·55
$\nu_{12} = \nu_{13}$	0·37

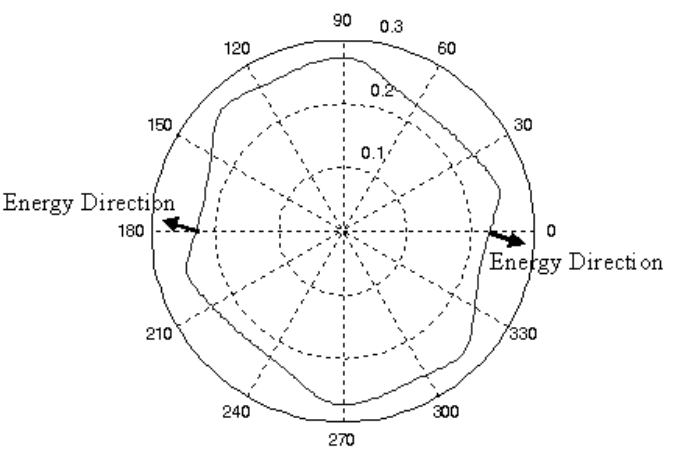


Figure 11. Slowness curve of the mode three at frequency 0·44MHz.

https://doi.org/10.1017/S0001924000003080 Published online by Cambridge University Press

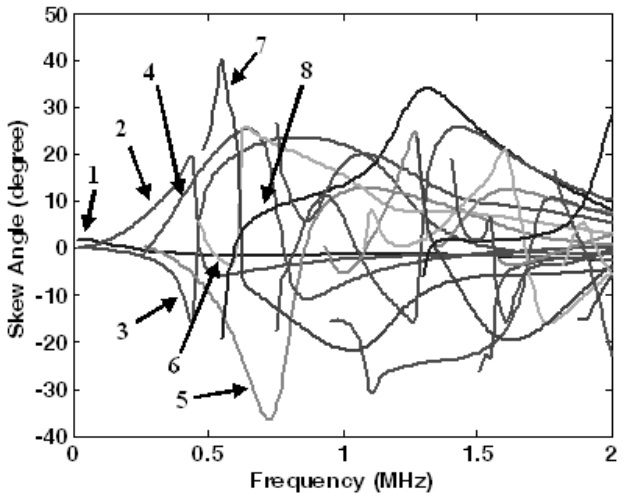


Figure 12. Skew angle dispersion curves of the 0° wave launching direction in the 16 layer quasi-isotropic plate.

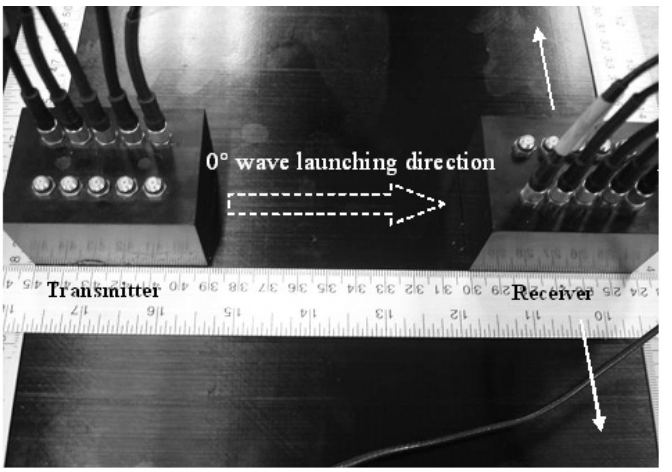
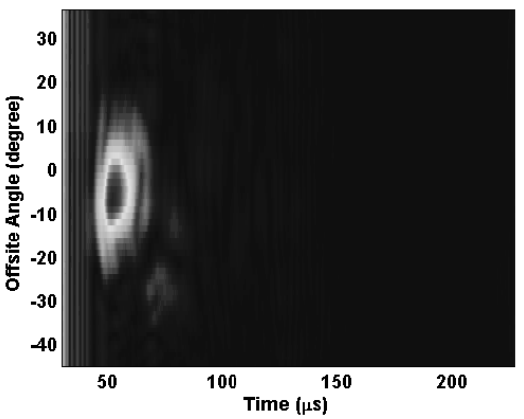
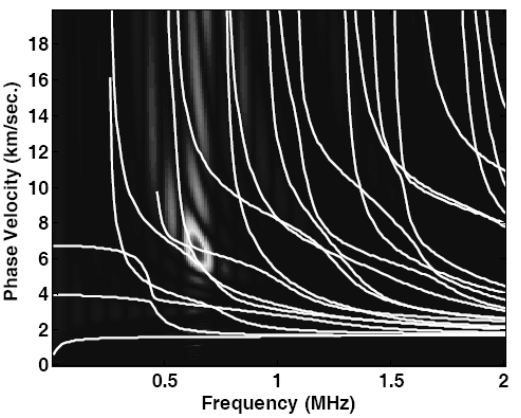


Figure 13. Experimental setup for the pitch-catch test on the composite plate.



(a) Signal amplitude map



(b) Excitation spectrum and dispersion curves

Figure 14. Signal amplitude map and the corresponding excitation spectrum for the 2·88μs time delay and the 0·65MHz 8 cycle tone-burst excitation, showing that the skew angle of the selected guided wave mode and frequency, mode 7 at 650kHz, is around –8°.

does not coincide with any directions of material symmetry. Moreover, the material anisotropy also introduces wave skew effects. When a wave skew effect takes place, the energy of the guided wave travels in a direction away from the wave launching direction. The angle from the wave launching direction to the wave energy propagation direction is the skew angle. The skew angle can be studied using the slowness curve based on the fact that the energy propagation direction is always perpendicular to the slowness curve[7,21]. Slowness is the reciprocal of the phase velocity. For composite plates, there is a unique slowness curve for each point of the dispersion curves.

Dispersion curves of a 16 layer quasi-isotropic carbon/epoxy composite plate are shown in Fig. 10 for the wave launching direction of 0°. The plate is made from Cytec CYCOM 977-3 carbon epoxy prepregs whose material properties are given in Table 1. The lay-up sequence of the plate is $[(0/45/90/-45)_s]_2$. The thickness of each ply is 0·2mm and the density of the plate is 1·608g/cm^3. The angle of the wave launching direction is defined by the angle between the direction of the 0 degree fibres and the wave launching direction. The guided wave modes are labeled based on the wave mode numbering system for composites proposed in Ref 19. The three fundamental modes with no cut-off frequencies are named mode one to three based on the values of phase velocities at low frequency. Higher order modes starting from mode four are numbered based on their cut-off frequencies for the 0° wave vector direction.

Use mode three at frequency 0·44MHz as an example. By tracking the slowness changes of this mode and frequency with respect to the changes of the wave launching direction, the slowness curve is obtained and plotted in a polar co-ordinate system as shown in Fig. 11. As it appears in this case, although a so-called quasi-isotropic lay-up is used for the composite plate, the phase velocity varies significantly from one wave launching direction to another. Based on the slowness curve, the energy propagation directions for the 0° and 180° wave launching directions are determined and marked with black arrows in the figure. The skew angles for the two wave launching directions, as can be seen, are of opposite values. As a result, if there is a defect in the path of the energy propagation when sending the guided wave to the 0° direction, the reflected guided wave with its wave launching direction in the 180° direction, will propagate back to the wave sending position. It is not hard to find out from the slowness curve that such a scenario is always true for any other wave launching directions. Therefore, it is possible to inspect the composite plate in different directions by exciting guided waves with different skew angles,

https://doi.org/10.1017/S0001924000003080 Published online by Cambridge University Press

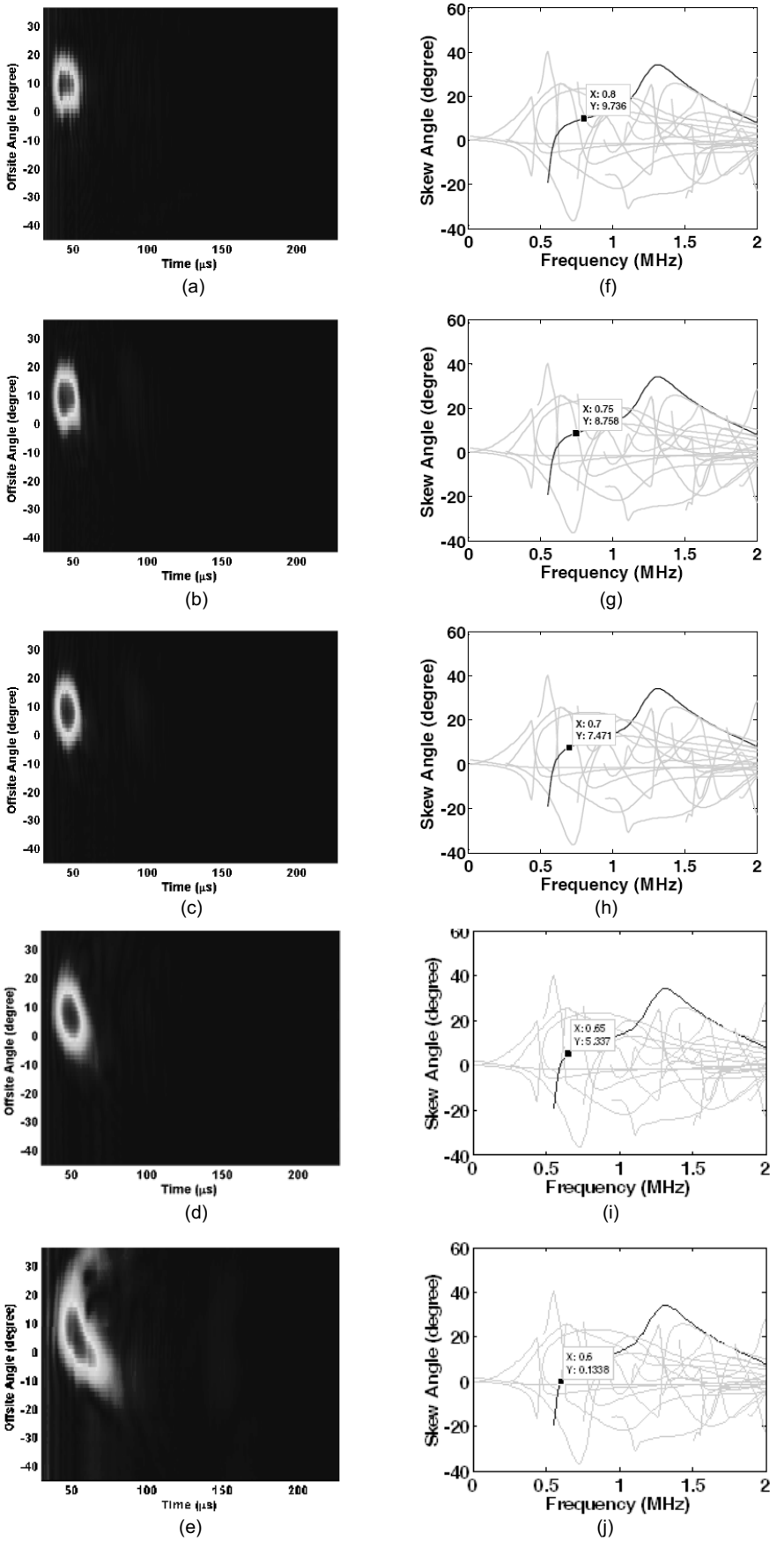


Figure 15. Signal amplitude maps and the corresponding skew angles for the mode eight at the frequencies (a) and (f): 0·8MHz; (b) and (g): 0·75MHz; (c) and (h): 0·7MHz; (d) and (i): 0·65MHz; (e) and (j): 0·6MHz.

https://doi.org/10.1017/S0001924000003080 Published online by Cambridge University Press

without changing the wave launching direction. This is of particular interest in structural health monitoring (SHM) applications in which rotating transducers to change the wave launching directions is usually not feasible.

It is apparent that knowing the skew angles for different wave modes and frequencies is essential for inspecting a composite plate using the wave skew effects. As to be presented next, the skew angles can be derived if the knowledge of the material properties, the lay-up sequence of the composite plate, and the thickness of each layer is known. The proposed skew effects based composite inspection technique is therefore different from the blind discontinuity inspection technique for isotropic plates in that necessary information of the composite plate for generating dispersion curves and obtaining skew angles is required.

The skew angles can be determined from the slowness curves. However, to obtain the slowness curves, one needs to calculate the phase velocities for all different wave launching directions. Besides, the numerical differentiation that is required to find the energy directions from the slowness curve is prone to numerical instability. An alternative way of calculating the skew angles is to use the Poynting vectors which are the power flow density vectors of the guided wave modes. The Poynting vector is defined as[21]:

$$\mathbf{P} = -\frac{\tilde{\mathbf{v}} \cdot \mathbf{T}}{2}. \qquad \ldots (21)$$

For plate wave guides, the three components of the Poyntg vector provides us with the power flow densities of a guided wave mode in three orthogonal directions. Since the wave launching direction is the x direction, the skew angle for the energy propagation is the angle of the power flow vector in the x-y plane and hence can be calculated based on the equation given below:

$$\varphi_{skew} = \mathrm{Tan}^{-1}\left(\frac{\int_{-h/2}^{h/2} P_y \mathrm{d}z}{\int_{-h/2}^{h/2} P_x \mathrm{d}z}\right). \qquad \ldots (22)$$

The skew angle of a certain mode and frequency can be directly calculated with Equation (22) once the particle velocity vector and the stress field are solved. Comparing to the slowness curve based skew angle calculation, the Poynting vector based method avoids the tedious phase velocity calculations for all wave launching directions as well as the numerical differentiations, and therefore is easier to implement and more stable. By evaluating Equation (22) for each point of the dispersion curves, the skew angle dispersion curves can be obtained. The skew angle dispersion curves that correspond to the dispersion curves shown in Fig. 10 are given in Fig. 12.

As shown, the skew angles for the 0° wave launching direction occupy a large angle range, approximately from –38° to 40°. Apparently, if a transducer is used to launch guided waves in the 0° direction, the guided wave energies could possibly propagate in any directions in the skew angle range. The large range of skew angles is a challenge for most guided wave based inspection techniques, especially when the defect locations are to be determined. However, the composite inspection technique proposed in this paper takes advantage of this large skew angle range. Any direction in the plate that is covered by the skew angle range can be inspected by selecting the guided wave mode and frequency whose skew angle matches the direction to be inspected. The time delay comb transducers provide us with a very good mode selection method, with which the mode and frequency tuning can be achieved electronically. In the next section, the feasibility of utilising the guided wave skew effects in the composite plate inspections is studied experimentally. The excitation spectrum and the skew angle dispersion curves serve as the theoretical foundation for the experiments.

7.0 EXPERIMENTS ON A COMPOSITE PLATE

The pitch-catch setup of the comb transducers shown in Fig. 5 was also employed in the experiment on the 16 layer composite plate to demonstrate the mode selection capability of the comb transducer as well as the skew effects of the guided wave propagations in the composite plate. The dispersion curves and the skew angle dispersion curves of the composite plate for the 0° wave launching direction are already given in Figs 10 and 12, respectively. In the experiments, the transmitter was fixed to ensure the 0° wave launching while the receiver was moved step by step perpendicular to the wave launching direction. A picture of the experimental setup is shown in Fig. 13. The receiver moving directions are marked with white solid arrows. The guided wave signals were recorded for every positions of the receiver. Since the angles offset from the wave launching direction can be calculated for the receiver positions, signal amplitude maps can be generated by plotting the signal envelopes against the corresponding offset angles.

The signal amplitude maps were generated for different excitation signals and time delay settings. Fig. 14(a) presents the signal amplitude map obtained when the time delay 2·88μs and the 0·65MHz 8 cycle tone-burst signal were used. The superposition of the excitation spectrum and the dispersion curves given in Fig. 14(b) shows that mode 7 was selected by the time delay and the excitation signal. From the skew angle dispersion curves, one can see that the skew angle of mode 7 at 0·65MHz is –8·5°. The offset angle at which the maximum signal amplitude was obtained, determined from Fig. 14(a), was –8·3°. Therefore, the experimental result matched with the theoretical prediction quite well.

The next step in the experiment was taken to see whether it was feasible to tune the wave energy propagation direction by applying different time delays and excitation signals to the time delay comb transducer. Mode 8 was selected in the experiment. The time delays and the centre frequency of the eight cycle tone-burst signals were varied for the purpose of selecting mode 8 at different frequencies. The signal amplitude maps for the frequencies 0·8MHz, 075MHz, 0·7MHz, 0·65MHz, and 0·6MHz are shown in Fig. 15(a) to Fig. 15(e), respectively. The corresponding skew angles are indicated from the highlighted skew angle curve of mode 8 and shown in Fig. 15(f) to Fig. 15(j), where X denotes the frequency in MHz and Y denotes the skew angle in degrees. It was demonstrated in Fig. 15 that the offset angle for receiving the maximum signal amplitude was shifted from around 9° to about 0°. Obviously, the wave energy propagation direction was successfully controlled by the time delay comb transducer. With the capability of controlling the wave energy propagation direction, the time delay comb transducer can be used to scan the composite plate in different directions.

8.0 CONCLUDING REMARKS

Time delay comb transducers are introduced as a promising tool for aircraft inspections. The investigation on the excitation spectrums of time delay comb transducers has demonstrated that ultrasonic guided wave mode tuning can be achieved. Based on the time delay and frequency tuning of the comb transducer, the discontinuity detections of isotropic objects whose exact material properties or thicknesses are unknown can still be conducted. This is especially suitable for aircraft inspections since some aircraft components have uncertain properties and thicknesses caused by poor records, applied painting layers, or other reasons. Guided wave propagations in fibre-reinforced composite plates are discussed with emphasis placed on the wave skew effects. Skew angle dispersion curves are generated using the Poynting vector based method. Combining the excitation spectrums of the time delay comb transducers together with the skew angle dispersion curves, we developed a skew angle based composite inspection technique. It is shown that, by using the time delay comb transducers, the guided wave energy can be sent to different directions with the aid of the wave skew

https://doi.org/10.1017/S0001924000003080 Published online by Cambridge University Press

effects to inspect the composite plate. However, to correctly locate the angular directions of the possible defects, the differences in the wave excitability and the sensitivity to defects of the guided waves that are sent to different directions must be taken into account. The exact amplitudes of the guided waves being sent to different directions can be determined after considering the wave excitabilities. The sensitivity study, on the other hand, offers the tool for quantitatively determining the amplitudes of the defect reflections. Putting the excitability and sensitivity studies together, one can fully interpret the reflection signals for different inspection directions and thus obtain a correct defect map for the composite plate under inspection. Research work on further development of the skew angle based composite inspection technique is undertaken. Finally, it is worth mentioning that the time delay control circuits may be eliminated by applying the time delays with a synthetic approach. In the synthetic approach, instead of exciting all elements of the transducer together with a time delay profile, only one element is excited at a time. The guided wave signals are received and recorded by all of the transducer elements. The excitation signal is switched from one element to another until all transducer elements are used as the wave excitation source for once. All of the recorded signals are then synthesised with appropriate time delays in a post-processing manner. Time delay control circuits are not required in a synthetic approach. For linear, noise-free application environments, the synthetic approach yields the same inspection results as the real-time approach does.

ACKNOWLEDGEMENTS

The authors would like to thank FBS Inc. and the National Science Foundation for the support of the phased array sensor and instrumentation work under Grant #IIP-0712301, and also AFOSR for the support of the composite material portion of this work under STTR Grant #FA9550-08-1-0311 through Dr Victor Giurgiutiu. Thanks are also given to Roger L. Royer, Russell Love, and Steven E. Owens in FBS Inc. for their help on the preparation of the experiments.

REFERENCES

1. ROSE, J.L. A baseline and version of ultrasonic guided wave inspection potential, 2002, *ASME J Pressure Vessel Technol*, **124**, pp 273-282.
2. ROSE, J.L. and SOLEY, L. Ultrasonic guided waves for the detection of anomalies in aircraft components, 2000, *Materials Evaluation*, **50**, pp 1080-1086.
3. MAL, M. and CHANG, Z. NDE of rivet holes in aging aircraft components using Lamb waves, 1998, Proc SPIE 3397, pp 68-75.
4. LANZA DI SCALEA, F., ROBINSON, J., TUZZEO, D. and BONOMO, M. Guided wave ultrasonics for NDE of aging aircraft components, 2002, Proc. SPIE 4704, pp 123-132.
5. ROYER, R.L. JR, ZHAO, X., OWENS, S.E. and ROSE, J.L. Large area corrosion detection in complex aircraft components using Lamb wave tomography, Proceedings, 6th International Workshop on Structural Health Monitoring, 2007, 11-13 September 2007, pp 238-246.
6. GIURGIUTIU, V., ZAGRAI, A. and BAO, J. Damage identification in aging aircraft structures with piezoelectric wafer active sensors, *J Intelligent Material Systems and Structures*, 2004, **15**, (9), pp 673-687.
7. ROSE, J.L. Ultrasonic waves in solid media cambridge university press, 1999, New York, NY, USA.
8. DITRI, J.J. and ROSE, J.L. Excitation of guided waves in generally anisotropic layers using finite source, 1994, *ASME J Appl Mech 61*, pp 330-338.
9. SANTONI, G.B., YU, L., XU, B. and GIURGIUTIU, V. Lamb wave mode tuning of piezoelectric wafer active sensors for structural health monitoring, *ASME J Vibration and Acoustics*, 2007, **129**, (6) pp 752-762.
10. RAGHAVAN, A. and CESNIK, C.E.S. Modeling of piezoelectric-based Lamb wave generation and sensing for structural health monitoring, 2004, Proc. of SPIE Vol. 5391, pp 419-430.
11. QUARRY, M.J. and ROSE, J.L. Multimode guided wave inspection of piping using comb transducers, *Materials Evaluation*, 1997, **45**, pp 504-508.
12. QUARRY, M. A Time Delay Comb Transducer for Guided Wave Mode Tuning in Piping, PhD Thesis, 2000, Pennsylvania State University, University Park, PA, USA.
13. LI, J. and ROSE, J.L. Implementing guided wave mode control by use of a phased transducer array, *IEEE Trans Ultrasonics Ferroelectron. Frequency Contr*, 2001, **48**, pp 761-768.
14. HAY, T.R. Aspects of Guided Waves in Structural Health Monitoring, PhD Thesis, 2004, Pennsylvania State University, University Park, PA, USA.
15. RHEINFRANK JR. G.B. and NORMAN W.A. Application of glass laminates to aircraft, 1944, *Mod Plastics*, **21**, pp 94-99.
16. DANIEL, I.M. and ISHAI, O. *Engineering Mechanics of Composite Materials*, 1994, 2nd ed, Oxford University Press.
17. NAYFEH, A.H. *Propagation in Layered Anisotropic Media with Application to Composites*, 1995, North Holland, Amsterdam, Netherlands.
18. BALASUBRAMANIAM, K. and KRISHNANMURTHY, C.V. Ultrasonic guided wave energy behavior in laminated anisotropic plates, 2006, *J Sound and Vibration*, **296**, pp 968-978.
19. GAO, H. Ultrasonic Guided Wave Mechanics for Composite Material Structural Health Monitoring, 2007, PhD Thesis, Pennsylvania State University, University Park, PA, USA.
20. YAN, F. AND ROSE, J.L. Guided wave phased array beam steering in composite plates, 2007, Proc. SPIE Vol 6532, pp 65320G.
21. AULD, B.A. Acoustic Fields and Waves in Solids, 1990, 2nd ed, Malabar, FL: KREIGER.
22. KIRRMANN, P. On the completeness of Lamb modes, *J Elasticity*, 1995, **37**, pp 39-39.
23. THOMSON, W.T. Transmission of elastic waves through a stratified solid medium, *J Applied Physics*, 1950, **21**, pp 89-93.
24. KNOPOFF, L. A matrix method for elastic wave problems, *Bull Seism Soc Am*, 1964, **54**, pp 431-438.
25. LOWE, M.J.S. Matrix techniques for modeling ultrasonic waves in multilayered media, IEEE Trans. Ultrason. Ferroelec. FrEquation Contr, 1995, **42**, (4), pp 525-542.
26. HAYASHI, T., SONG, W.J. and ROSE, L.J. Guided wave dispersion curves for a bar with an arbitrary cross-section, a rod and rail example, *Ultrasonics*, 2003, **41**, (3), pp 175-183.

https://doi.org/10.1017/S0001924000003080 Published online by Cambridge University Press